Shahrood University of Technology

Journal of Hydraulic and Water Engineering (JHWE)

Journal homepage: https://jhwe.shahroodut.ac.ir/

Iranian Hydraulic Association (IHA)

Comparison of the Impact of Akmon, Sta-bar, Sta-pod, Stock cube, and Tribar Armoring Layers on the Level of Flow Rate and Wave Overtopping

A. Safari [1], M. Behdarvandi Askar [2,*]

[1] Master's student of Civil Engineering, Coastal, Ports and Marine Structures, Khorramshahr University of Marine Science and Technology, Khorramshahr, Iran.
[2] Associate professor of Department of Marine Structures Khorramshahr University of Marine Science and Technology, Khorramshahr, Iran

Article Info

Article history:

Received: 18 March 2023
Received in revised form: 10 April 2023
Accepted:23 August 2023
Published online: 25 August 2023

DOI:
10.22044/JHWE.2023.12858.1007

Keywords
Layer armor
Breakwater
Wave
FLOW-3D software
discharge capacity
crest height.

Abstract

Breakwaters are structuring whose main function is to reduce waves in an area and create a calm basin for the stopping, movement, and maneuvering of floating objects. Concrete armors can be constructed in different shapes, allowing for the creation of armors that have high engagement properties and an increased damage coefficient (KD), ultimately leading to a reduction in the weight of armor pieces and their ability to be deployed in steeper slopes on the breakwater body. Most coastal protection structures built in the country are of the traditional rubble and platform type, and the structures made with concrete armor are few and far between. In this study, the impact of Akmon, Sta-bar, Sta-pod, Stock cube, and Tribar armoring layers on the level of flow rate and wave overtopping in coastal protection structures and which type of armor has the least overflow is investigated. First, the overall geometry of the breakwater and then the geometry of each armor layer are separately drawn using AutoCAD software and prepared for calling to the main model, the FLOW-3D 11.0.4 software. After modeling, the results are analyzed through the main model and Excel software. The lowest wave overtopping in the breakwater occurs in the Akmon armor state, and the highest wave overtopping in the breakwater occurs in the Stock Cube armor layer state. The lowest flow rate among breakwaters occurred in the Akmon armor state, and the highest flow rate among the five breakwaters also occurred in the Stock Cube armor state, which is approximately 6 times higher than the minimum state.

1. Introduction

Breakwaters are structures that are built to create calmness in ports, ensure the safe entry of ships into waterways and ports, reduce the energy of waves, and protect coasts against waves (Ehrlich and Kulhawy, 1982). Breakwaters are classified into various types based on different aspects such as geometric shape, materials used, and their placement (Dai et al., 2018). Among the various types of breakwaters based on geometric shape and materials used, rubble mound breakwaters are one of the most common types.

* *Corresponding author:* sazehenteghal@yahoo.com

In recent decades, the design and construction of flexible breakwaters have increased in many parts of the world (McCartney, 1985). These structures undergo deformation under the impact of sea waves and, after deformation, reach static or dynamic stability based on environmental and structural conditions. In the design of these structures, the belief that the protective layer materials of the structure must be stable against wave attacks is violated, allowing the structure to continue to deform until it reaches a more effective form. In the implementation of such structures, due to the permissible deformation of the structure, a wider range of stone mining materials can be used, and with regard to their performance philosophy in facing sea waves, materials with less tonnage can also be used.

The presence of a platform in flexible structures leads to a further reduction of wave energy compared to other flexible structures. Other advantages of this type of breakwater compared to other types of mass concrete breakwaters include reducing wave overtopping on the top of the standing surface, reducing wave spillage over the structure, easy implementation of these structures due to limited facilities, lighter machinery, and local contractor experiences. Additionally, due to the permissible deformation of these structures, optimal use of stone mines in a wider range of materials is possible. Figure 1 shows an example of this type of breakwater (Kim, 2010).

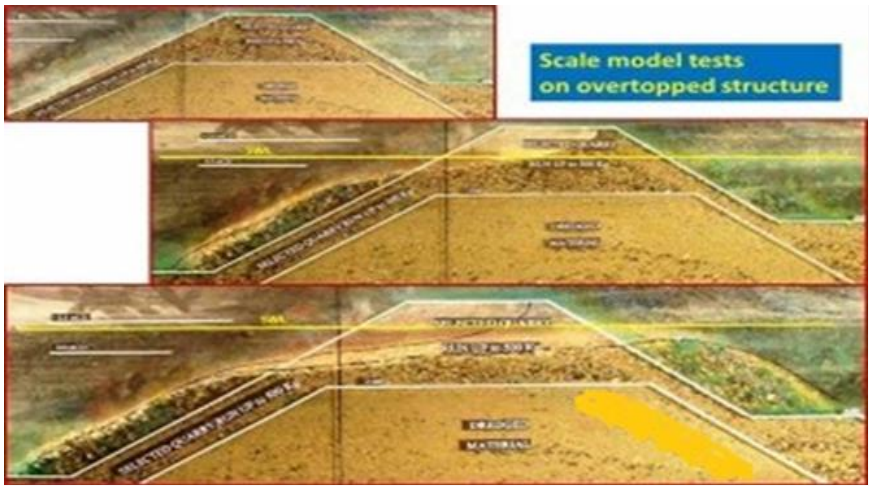

Figure 1. An example of a flexible breakwater.

The stability of a rubble mound breakwater depends on various factors, including the appearance of the armor stones and their specific weight, the method of execution of the foundation and the breakwater layers, the geometric status of the structure, the slope angle, and the crest height. In the following, some explanations regarding the design issues of rubble mound breakwaters are presented briefly (Elchahal et al., 2009; Kim, 2010).

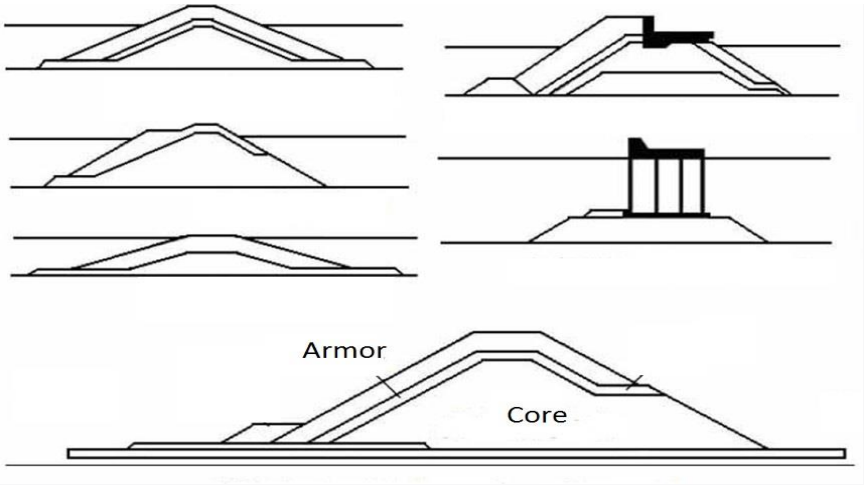

Figure 2. Different types of breakwaters in terms of their structure.

As mentioned, rubble-mound breakwaters are the most common type of breakwater constructed worldwide. These breakwaters are made using either quarry rock or concrete units. Rubble-mound breakwaters have excellent wave absorption properties and, due to their geometric shape and structure, they are highly stable and have a very long lifespan (Briganti et al., 2022).

Some of the advantages of this type of breakwater include: the rock materials are usually locally available; the construction of these structures is relatively simple and can be done with basic equipment; the deterioration of these structures occurs gradually and can be repaired at different stages; the structure has the necessary flexibility to withstand wave conditions beyond the designed wave height; and the structure is not very sensitive to various settlements due to its flexibility properties (Sumer and Fredsøe, 2000; Van der Meer, 1995).

Since the volume of materials used in breakwaters and coastal protection projects is usually very high, rocks are considered one of the most practical and essential materials used in these projects to reduce the risk of structural failure (Ali and Diwedar, 2014).

The main criteria for selecting rocks in such projects include resistance, durability, blockiness, physical properties, environmental compatibility, accessibility, execution conditions, transport, deployment, and environmental effects. Among these characteristics, rock durability and its resistance to destructive and aggressive factors prevailing in marine environments are among the most important properties that the materials used in the construction of marine structures must possess.

This study focuses on the characteristics of the Akmon, Sta-bar, Sta-pod, Stock cube, and Tribar armor layers, each of which has an impact on the amount of flow rate and wave overtopping in coastal protection structures, and which type of armor has the least amount of overflow, as shown in Figure 3.

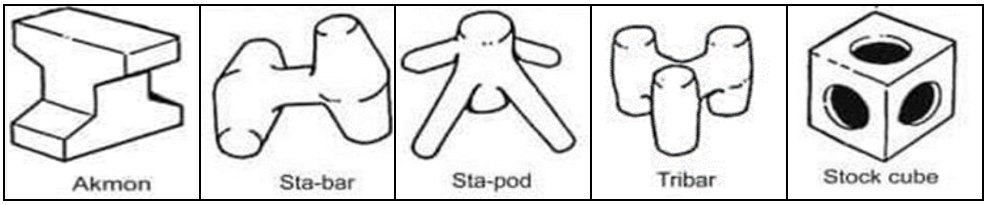

Figure 3. A representation of different types of armor.

Bruce et al. (2009) describe a primary program of physical model experiments at a small scale to better understand the effect of armor type and configuration on the upper surface behavior. In particular, 179 tests determined the relative differences in upper surface behavior for 13 types of armor. The roughness factors γ_f were determined for stone (two layers), cube (single and two layers), Tetrapod, Antifer, Haro, Accropode, Core-Loc™, and Xbloc™. These roughness factors are included in the CLASH database and are used for neural network prediction of the upper surface. The wave-by-wave analysis of the upper volumes was analyzed and compared well with current prediction methods. The measured reflection coefficients for various units are also presented and compared with recent formulas. Pepi et al. (2022) investigated the phenomenon of wave overtopping as a threat to mass concrete breakwaters designed to protect coastal areas or ports. The evaluation of wave overtopping for such structures is mostly done using empirical formulas that include hydraulic and geometric variables along with corrective factors such as armor roughness.

Prediction formulas for wave overtopping in sloping structures are usually applied assuming a constant value of this parameter based on the type of armor units, the number of layers, and the core type. They presented a new method for estimating the roughness coefficient of mass concrete breakwaters as a function of hydraulic and structural parameters.

A new method for estimating the roughness coefficient, based on the accurate geometric representation, presents an improved prediction of the mean flow rate compared to existing formulas. Qasemi and Shafiaifar (2014) presented a study on the calculation of wave run-up from the Xbloc armor breakwater. In this study, the FLOW-3D numerical model was used to investigate the run-up phenomenon, and the run-up rate was calculated and compared for precast Xbloc blocks under various sea conditions and regular and irregular armor arrangements. The results show that as the wave height and water depth increase, the run-up rate increases, particularly at low porosity ratios. By modeling for different slopes of the Xbloc breakwater geometry, it was observed that the run-up rate increases with higher wave heights and gentler slopes, whereas the run-up rate is significantly lower for steeper slopes.

2. Material and methods

Wave breaking is modeled using the hydraulic software FLOW-3D, and the effect of waves on the type of breakwater at the base of the structure is studied. FLOW-3D is a powerful CFD software designed, developed, and supported by Flow Science, Inc. This software is designed to help research the dynamic behavior of fluids and gases in a wide range of practical applications. FLOW-3D is designed for one-dimensional, two-dimensional, and three-dimensional problems.

In the steady state, results are obtained in a very short time because the program is based on the fundamental laws of mass, momentum, and energy conservation. FLOW-3D uses a network of rectangular elements, making modeling easy and regular, and requiring less memory for storage. The basis of the equations of motion in this software is the Finite Difference technique (FLOW-3D, 2013; Gandomi et al., 2022).

In this research, first, the general geometry of the breakwater and then the geometry of each layer of the armor are separately drawn using AutoCAD software and prepared for calling in the main model, namely FLOW-3D 11.0.4 software. After modeling, the results are analyzed using both the main model itself and Excel software. FLOW-3D software is one of the most well-known software for analyzing fluid flow by computational fluid dynamics method. In FLOW-3D, geometry, and

meshing of the problem are independent of each other, and three-dimensional modeling with complex geometry is easily done (FLOW-3D, 2013).

To calibrate and validate the numerical model, the laboratory studies of Bruce et al. (2009) were used. In this study, irregular waves with the Jonswap spectrum are incident on the outer layer, and flow velocity is measured using laboratory equipment. It should be noted that irregular waves are generated with the Jonswap spectrum and the maximum wave height is 12 centimeters, with a period of 1 second, colliding with the breakwater. For calibration and validation of the numerical model, the hydrodynamic parameters of the model, including period, wave height, and maximum energy spectrum values, are compared with the laboratory values to determine the numerical error accuracy in simulating hydrodynamic parameters. In this research, the armor layers of Akmon, Sta-bar, Sta-pod, Stock cube, and Tribar were studied to determine their impact on the flow rate and wave overtopping in coastal protection structures and to determine which type of armor has the least overflow. The transverse profile geometry of the breakwaters for modeling in FLOW-3D software is presented in the figure below.

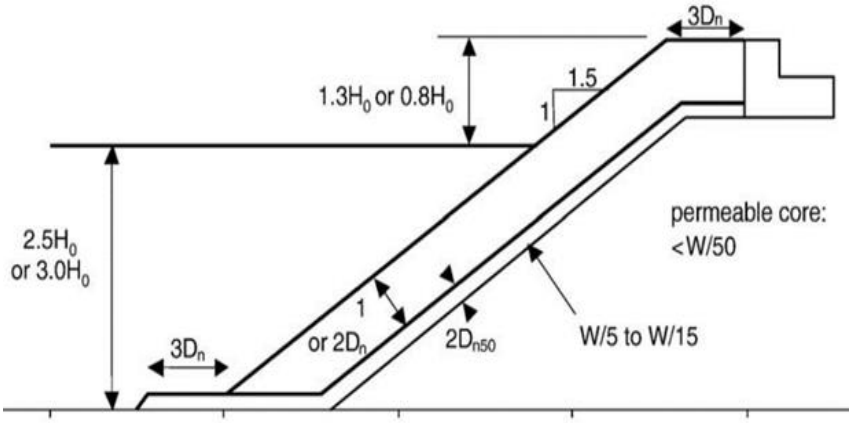

Figure 4. Information and geometric section of the wave breaker

Table 1. Information on the armor layers of the wave breaker.

	W_{50} [kg]	D_{n50} [m]	ρ [kg/m^3]	N_a [-]	N [-]	Δ [-]	H_0 [m]	h_s [m]	R_c [m]	B_t [m]	$W_{u,max}$ [kg]	$W_{u,min}$ [kg]	$W_{core,\ max}$ [kg]
Sta-bar	0.0620	0.030	2361	660	264	1.36	0.089	0.222	0.089	0.089	0.012	0.004	0.0012
Sta-pod	0.0850	0.033	2361	535	214	1.36	0.099	0.247	0.099	0.099	0.017	0.006	0.0017
Akmon	0.1000	0.035	2350	427	171	1.35	0.104	0.259	0.104	0.105	0.020	0.007	0.0020
Stock cube	0.0742	0.032	2361	622	249	1.36	0.107	0.268	0.107	0.095	0.015	0.005	0.0015
Tribar	0.0605	0.030	2300	632	253	1.30	0.108	0.271	0.108	0.089	0.012	0.004	0.0012

The length of the computational domain was considered based on the laboratory flume length of 10 meters, a width of 35 centimeters, and a height of 65 centimeters for the computational domain. To optimize the number of computational cells, a four-block grid was used for this 10-meter computational domain. One of the fundamental points to consider in numerical simulations is the application of boundary conditions.

After determining the computational domain with the above details, a boundary condition must be defined for each face of these four blocks. At the beginning of the first computational block, the wave boundary condition was used, and at all lower boundaries, the wall boundary condition was used at the end of the fourth block, the output boundary condition was used, and at other boundaries, the symmetry boundary condition was used. The only boundary condition that requires further explanation is the wave boundary condition used at the beginning of the first block because this modeling is intended to produce irregular waves similar to laboratory experiments.

To create the JONSWAP wave spectrum in the software, the input wave spectrum must be applied at the top boundary condition of the simulation channel. Given that various wave models are applicable in the FLOW-3D software, the required parameters for creating the JONSWAP wave conditions in the software include wind duration, wind speed at a height of 10 meters, and peak enhancement factor, which is one of the characteristics of the JONSWAP wave and is taken to be 3.3 on average.

Meshing, due to its direct impact on the modeling results, is one of the most important stages in the modeling process. Therefore, special attention is paid to the details of meshing. Proper meshing provides an optimal balance between good performance and accurate equation solving. If meshing is done with great precision, it will take a very long time to perform the calculations. In some cases, it has been observed that several months are required to perform calculations with detailed and accurate meshing.

On the other hand, meshing should have an accuracy such that the results obtained from modeling have an appropriate accuracy when compared to actual evidence. The time required to solve the problem depends on the accuracy of the meshing. The relationship between the time required to solve the problem and the size of the mesh is not entirely linear. If we double the number of cells between the meshes, the computation time will increase more than twice. Increasing the accuracy of the meshing should be done at the appropriate locations, such as input channels, thin walls, and areas where the probability of the occurrence of vortices exists.

It is important to pay special attention to meshing details because of its direct impact on modeling results. Proper meshing is the optimal balance between performance and accuracy of solving equations. If meshing is done with high accuracy, computation time will be very long.

In some cases, it has been observed that it takes several months to perform calculations with fine and accurate meshing. On the other hand, meshing should be accurate enough so that the results of modeling have an appropriate accuracy compared to real evidence. The problem-solving time depends on the accuracy of the meshing. The relationship between problem-solving time and mesh size is not completely linear. If we double the number of cells in the meshes, computation time will increase by more than double. Increasing the accuracy of meshing should be done in the appropriate locations, which are places where it is necessary to increase the accuracy, such as input channels, thin walls, and places where vortex occurrence is likely.

Avoid increasing mesh accuracy in places where high accuracy is not needed, such as templates, stairs, and open spaces.

It is better to start the calculation process with a coarse mesh and then perform the calculation again by increasing the mesh accuracy. This is recommended because, in the beginning, calculations should be done to see if simulation parameters have been properly introduced or not. It also allows for a general view of possible solutions.

To validate the numerical model created in the FLOW-3D software, the experimental sample of Bruce et al. (2009), shown in Figure 5, was simulated in the software. In this study, the R^2 coefficient of determination, mean absolute percentage error, and root mean square error were used to evaluate the model's accuracy.

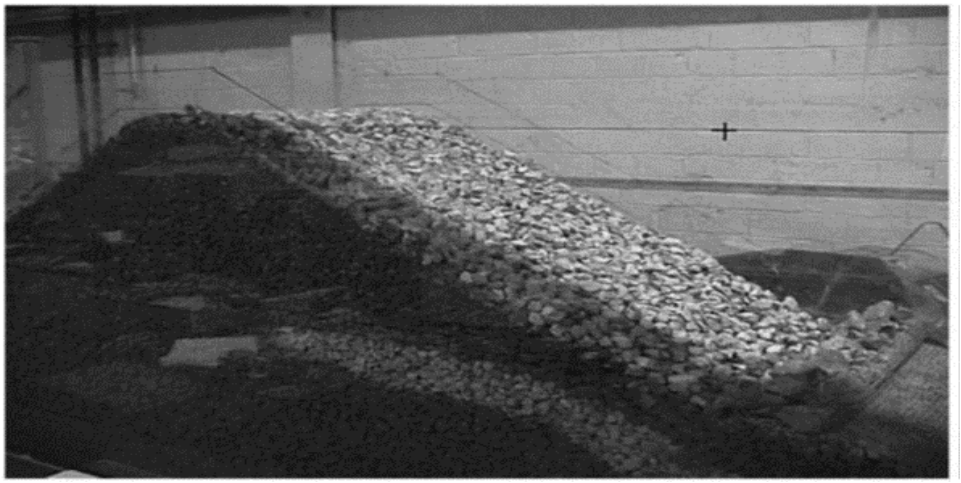

Figure 5. Laboratory experimental sample by Bruce et al. (2009)

The size of the cells in the mesh network has been selected in such a way that their values are small in the vicinity of the breakwater and become larger as they move away from the intended structure. It should be noted that the sensitivity analysis of cell sizes has been performed, and the most appropriate cell sizes for this case have been presented here.

Accordingly, the cell size was initially selected as 90 centimeters and then, by reducing its size to 2 centimeters over six stages, the numerical results were independent of cell size. The accuracy evaluation results of the numerical model based on the simulation of the breakwater geometry, water surface profile, wave height before and after the breakwater, and consequently, the calculation of the transmission coefficient under experimental conditions are presented. The comparison of the experimental values with the corresponding simulation results is shown in Figure 1.

Table 2. Attempt and error of validation.

Percentage of Error in Numerical and Laboratory Results (%)	Mesh Size (cm)
4.31%	2 cm
15.62%	5 cm
22.95%	10 cm
31.18%	40 cm

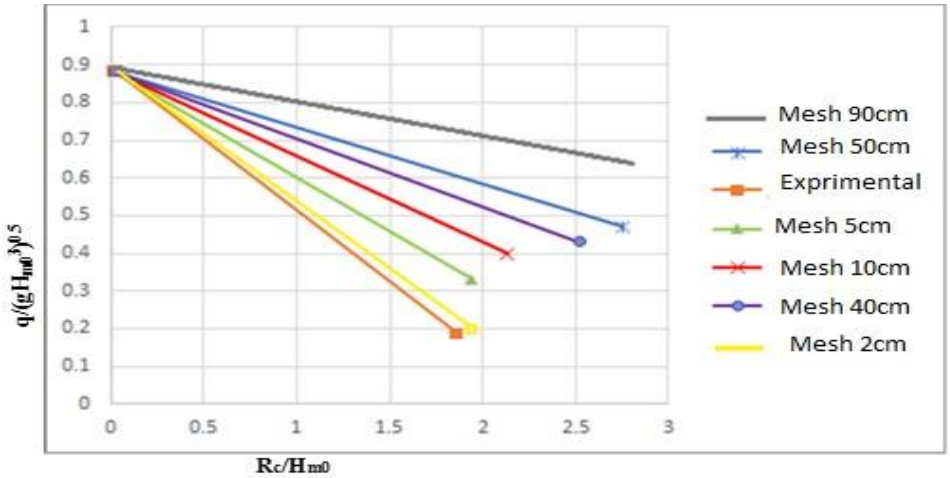

Figure 6. Validation graph of experimental and numerical analysis samples.

According to Figure 1, by reducing the mesh size from 5 centimeters to 2 centimeters, the error between the experimental results and the numerical software model decreased to about 4.31%.

3. Results and Discussion

As mentioned in the previous section, in this study, the performance and comparative behavioral analysis of Akmon, Sta-bar, Sta-pod, Stock cube, and Tribar armor layers, which affect the amount of wave overtopping and wave reflection on coastal protection structures, were modeled in FLOW-3D software. After modeling and analysis by FLOW-3D software, the following results were obtained.

After analysis and comparing the graphs of the wave transmission force (P) comparison for the breakwater (Akmon, Sta-bar, Sta-pod, Stock cube, Tribar), it is observed that in the breakwater sample (Stock cube state), the value of wave transmission force entering the upper body of the breakwater is about 18.6 Newton at a cycle time of 1 second.

In the breakwater sample (Tribar state), the maximum wave transmission force entering the upper body of the breakwater is about 18.3 Newton at a cycle time of 1 second, and in the breakwater sample (Sta-pod state), the maximum wave transmission force entering the upper body of the breakwater is about 16.3 Newton at a cycle time of 1 second. In addition, in the breakwater sample (Akmon state), the maximum wave transmission force entering the upper body of the breakwater is about 14.3 Newton at a cycle time of 1 second, and finally, the breakwater sample (Sta-bar state) has the maximum wave transmission force entering the upper body of the breakwater, which is about 15.9 Newton at a cycle time of 1 second. It is also observed that the highest wave transmission force is on the breakwater with the Stock cube armor state, and according to the comparison column graph of the wave transmission force, the lowest wave transmission force is in the Akmon armor state. Furthermore, by comparing the breakwaters with the Sta-bar, Sta-pod, and Tribar armor states, it was observed that the amount of wave transmission force on the breakwaters is very close to each other and have a very small difference from each other, which in a way. The performance of these three armor modes is very close to each other. As shown in the analysis results presented in the output, the highest wave transfer force occurs on the upper body of the stock cube wave breaker, and the lowest wave transfer force at a frequency of 1 second is related to the Akmon armor.

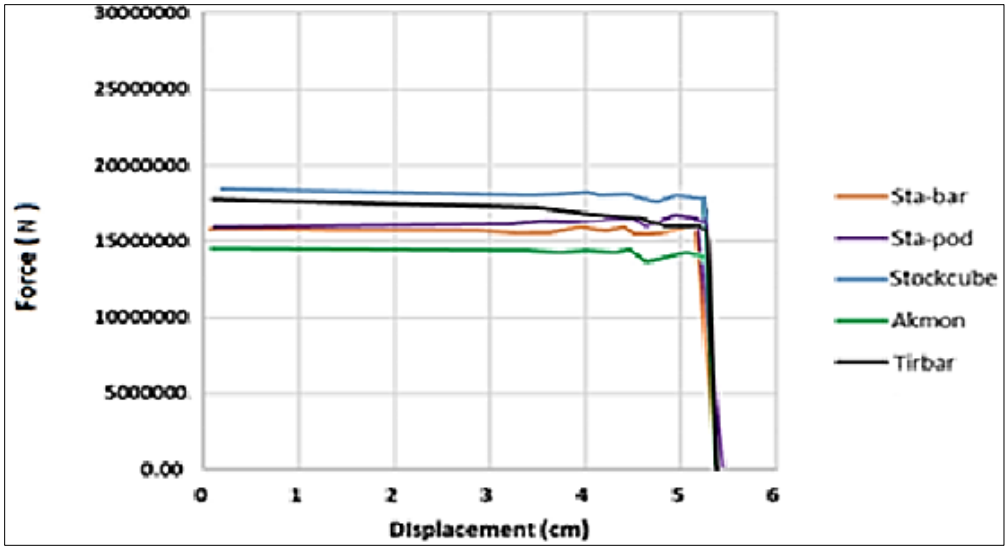

Figure 7. Comparison chart of wave transfer force (P) for wave breakers (Akmon, Sta-bar, Sta-pod, Stock cube, Tribar).

After analyzing and considering the wave speed comparison graph (V) in Figure 3 for the breakwaters (Akmon, Sta-bar, Sta-pod, Stock cube, Tribar), it can be observed that the breakwater with armor (Stock cube) has the highest wave speed of approximately 24.8 meters per second at a period of 2.95 seconds. Additionally, in the breakwater sample with armor (Tirbar), the highest wave speed is approximately 5.81 meters per second at a period of 4.869 seconds. Furthermore, in the sample of the breakwater with armor (Sta-pod), the highest wave speed is approximately 5.69 meters per second at a period of 11.2 seconds.

Finally, in the breakwater with armor (Akmon), the highest wave speed is approximately 5.41 meters per second at a period of 4.86 seconds. It is also observed from the analysis results for wave speed (V) for the five armor types of breakwaters (Akmon, Sta-bar, Sta-pod, Stock cube, Tribar) in Figure 3 that the highest wave speed is on the breakwater with the armor of Stock Cube. Based on the comparison column graph of wave speed, it is observed that the lowest wave speed is in the Akmon armor type. Moreover, by comparing the breakwaters with the armor types of Sta-Pod, Tribar, and Sta-bar, it is observed that the wave speed of the breakwaters is very close to each other, and they have very little difference in performance in terms of wave speed.

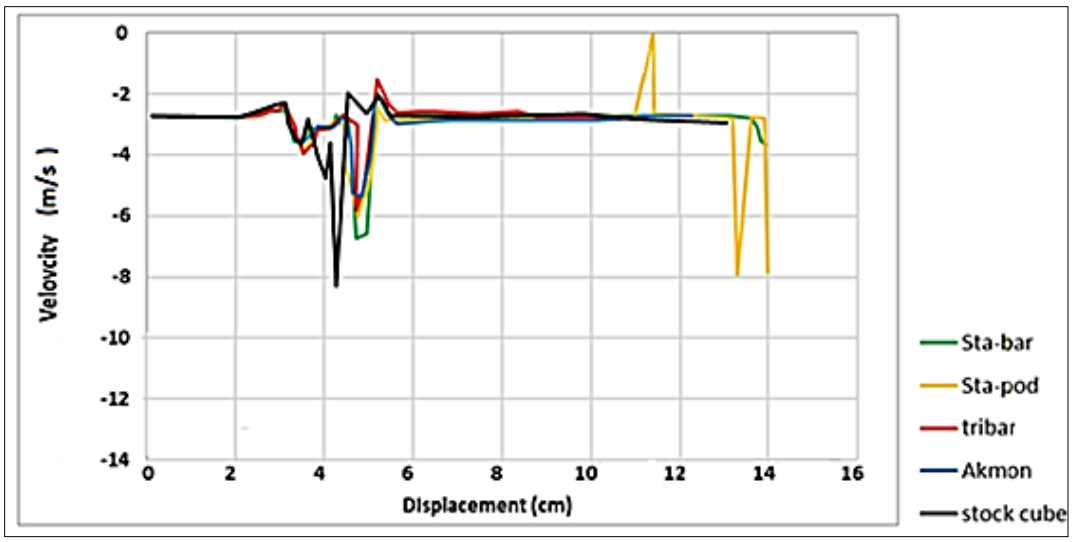

Figure 8. Comparison chart of wave velocity (V) for wave breakers (Akmon, Sta-bar, Sta-pod, Stock cube, Tribar).

After conducting an analysis and comparing the wave transmission coefficient (Q) comparison chart, chart 4 is observed for breakwaters with armor in the Akmon, Sta-bar, Sta-pod, Stock cube, and Tribar configurations.

In the breakwater with Stock cube armor, the wave transmission coefficient from the breakwater is approximately 179.0 cubic meters per second at an approximate period of 15 seconds. Additionally, in the sample breakwater with Tirbar armor, the wave transmission coefficient is approximately 12.0 cubic meters per second at an approximate period of 15 seconds. Furthermore, in the sample breakwater with Sta-pod armor, the wave transmission coefficient is approximately 0.69 cubic meters per second at an approximate period of 15 seconds.

In the breakwater with Akmon armor, the wave transmission coefficient is approximately 0.29 cubic meters per second at an approximate period of 15 seconds on the upper part of the breakwater. Lastly, in the breakwater with Sta-bar armor, the wave transmission coefficient is approximately 0.45 cubic meters per second at an approximate period of 15 seconds on the upper part of the breakwater.

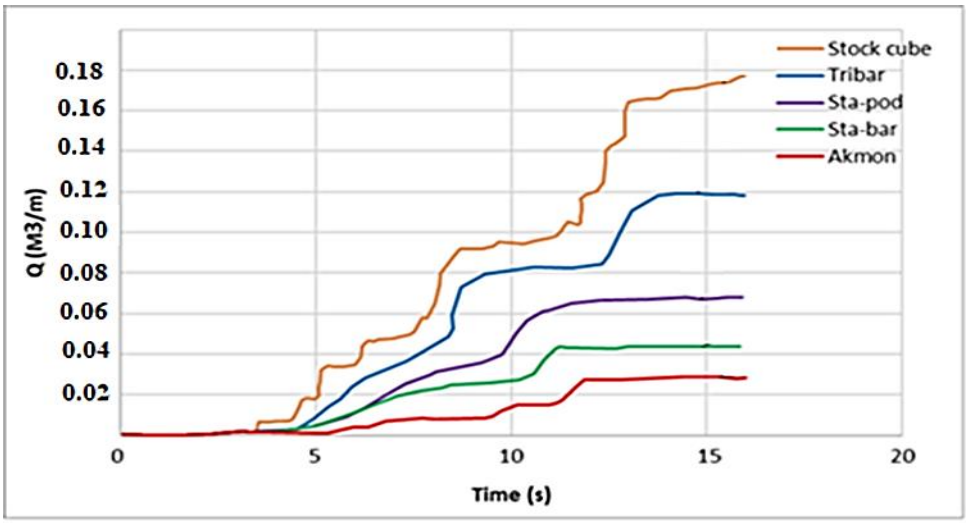

Figure 9. Comparison chart of wave discharge rates for different types of armor in wave breakers, including Akmon, Sta-bar, Sta-pod, Stock cube, and Tribar.

After conducting the analysis and considering the comparison chart of the wave height (E), Chart 5 is observed for armor breakwaters with the Akmon, Sta-bar, Sta-pod, Stock cube, and Tribar configurations. In the armor breakwater with the Stock cube configuration, the height of the wave crest is about 24.0 meters from the breakwater at an approximate period of 7.3 seconds. Additionally, in the armor breakwater with the Tribar configuration, the height of the wave crest is about 20.0 meters from the breakwater at an approximate period of 63.4 seconds. Furthermore, in the armor breakwater with the Sta-pod configuration, the height of the wave crest is about 14.0 meters from the breakwater at an approximate period of 4.5 seconds. In the armor breakwater with the Akmon configuration, the height of the wave crest is about 10.0 meters from the breakwater at a period of approximately 7.5 seconds. Lastly, in the armor breakwater with the Sta-bar configuration, the height of the wave crest is about 18.0 meters from the breakwater at an approximate period of 7.4 seconds.

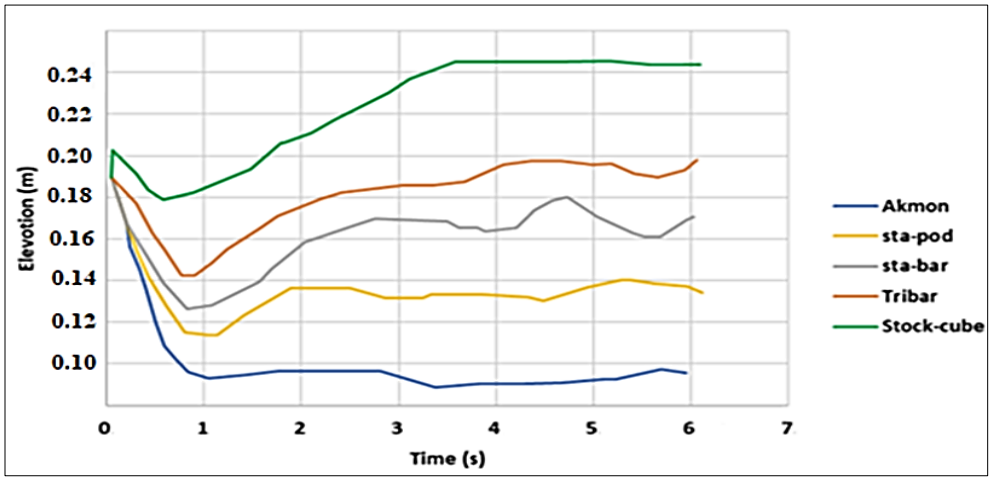

Figure 10. Comparison chart of wave crest height on breakwaters (Akmon, Sta-bar, Sta-pod, Stock cube, Tribar).

As observed, the Akmon armor layer has a better performance compared to other armor layers, which is shown as a percentage in Table 3.

Table 3. Performance of Akmon armor layer compared to Stock cube, Sta-bar, Sta-pod, and Tribar armor layers.

	Stock cube	Sta-bar	Sta-pod	Tribar
Force	100%	21.2	12.98	29.47
Velocity	42.32	25.91	9.29	8.41
Overtopping	484.20	57.14	142.85	328.57
Wave run-up	18.5	11	7	12.5

4. Conclusions

Based on the obtained results, this section will focus on the conclusion and recommendations for future studies. After performing numerical analysis using the FLOW-3D finite element software and calculating and examining the effects of the armor layer and protective layer, the results are presented below:

According to the wave transmission force (P) graph of the (Stock cube) state wave breaker, the wave transmission force (P) was about 17.6 Newtons during a specific period.

According to the wave transmission force (P) graph of the (Akmon) state wave breaker, the wave transmission force (P) was the lowest among the other armor layers during a specific period, which was about 14.3 Newtons.

Comparing the wave transmission force (P) graph of the (Sta-pod) state wave breaker with the (Tribar) state wave breaker during a specific period, it performed better and the force exerted on the body due to the wave impact was about 16.3 Newtons.

Based on these findings, it is recommended that further studies be conducted to optimize the design of wave breakers and improve their performance.

Based on the comparison of the wave transmission force (P) graph between the Sta-bar state breaker and Sta-pod state breaker during a specific time period, it has been shown that the Sta-bar performs better and exerts a force on the body due to the wave impact of approximately 9.15 Newtons. In a way, the behavior of these two breakers is very similar and they have almost the same performance.

In a similar comparison of the wave transmission force (P) graph between the Sta-bar state breaker and Tribar state breaker during a specific time period, it has been shown that the Sta-bar performs better and exerts a force on the body due to the wave impact of approximately 9.15 Newtons.

The highest wave transmission speed on the armor Stock Cube breaker at a cycle time of 2.95 seconds is approximately 24.8 meters per second on the upper body of the breaker. The lowest wave transmission speed is observed in the armor Akmon state breaker at a cycle time of 4.86 seconds with an impact force of about 5.41 meters per second on the upper body of the breaker. By comparing the breakers with the Sta-Pod, Tribar, and Sta-bar armor states, it was observed that the speed of wave transmission on the breakers is very close to each other and they have very little difference in performance.

The lowest wave impact on the breaker occurs in the armor Akmon state, where the height of the wave above the breaker at a cycle time of approximately 5.7 seconds is

about 10.0 meters. The highest wave impact occurs in the Stock Cube armor state breaker, where the height of the wave above the breaker at a cycle time of 3.7 seconds is about 24.0 meters. In the Tribar armor state breaker, the height of the wave above the breaker at a cycle time of approximately 4.63 seconds is about 20.0 meters. In the Sta-pod armor state breaker, the highest wave height above the breaker at a cycle time of approximately 4.5 seconds is about 14.0 meters.

Data Availability

The data used to support the findings of this study is available from the corresponding author upon request.

Conflicts of Interest

The authors declare that they have no conflicts of interest regarding the publication of this paper.

References

Ali, A.M., A., Diwedar, A.S., 2014. Double-layer armor breakwater stability (case study: El Dikheila Port, Alexandria, Egypt). Ain Shams Engineering Journal, 5(3): 681-689.

Briganti, R. et al., 2022. Wave overtopping at near-vertical seawalls: Influence of foreshore evolution during storms. Ocean Engineering, 261: 112024.

Bruce, T., Van der Meer, J., Franco, L., Pearson, J.M., 2009. Overtopping performance of different armor units for rubble mound breakwaters. Coastal Engineering, 56(2): 166-179.

Dai, J., Wang, C.M., Utsunomiya, T., Duan, W., 2018. Review of recent research and developments on floating breakwaters. Ocean Engineering, 158: 132-151.

Ehrlich, L.A., Kulhawy, F.H., 1982. COASTAL STRUCTURES HANDBOOK SERIES BREAKWATERS, JETTIES AND GROINS.

Elchahal, G., Lafon, P., Younes, R., 2009. Design optimization of floating breakwaters with an interdisciplinary fluid–solid structural problem. Canadian journal of civil engineering, 36(11): 1732-1743.

FLOW-3D, 2013. User Manual, version 11.0.3; Flow Science, Inc.: Santa Fe, NM, USA.

Gandomi, M.Ů., Solimani Babarsad, M., Pourmohammadi, M.H., Ghorbanizadeh Kharrazi, H., Derikvand, E., 2022. Simulation of Ogee Spillway by FLOW3D Software (Case Study: Shahid Abbaspour Dam). Journal of Hydraulic Structures, 8(3): 88-107.

Kim, Y.C., 2010. Handbook of coastal and ocean engineering. World Scientific.

McCartney, B.L., 1985. Floating breakwater design. Journal of Waterway, Port, Coastal, and Ocean Engineering, 111(2): 304-318.

Pepi, Y., Romano, A., Franco, L., 2022. Wave overtopping at rubble mound breakwaters: A new method to estimate roughness factor for rock armours under non-breaking waves. Coastal Engineering, 178: 104197.

Sumer, B.M., Fredsøe, J., 2000. Experimental study of 2D scour and its protection at a rubble-mound breakwater. Coastal Engineering, 40(1): 59-87.

Van der Meer, J.W., 1995. Conceptual design of rubble mound breakwaters, Advances In Coastal And Ocean Engineering: (Volume 1). World Scientific, pp. 221-315.